

MOC2DIMES: A CAMERA SIMULATOR FOR THE MARS EXPLORATION ROVER DESCENT IMAGE MOTION ESTIMATION SYSTEM

Reg G. Willson, Andrew E. Johnson, Jay D. Goguen

*Jet Propulsion Laboratory, California Institute of Technology,
4800 Oak Grove Drive, Pasadena, CA 91109, USA
Email: {reg.willson, aej, jay.goguen}@jpl.nasa.gov*

ABSTRACT

Camera simulators can generate images for developing algorithms, tuning parameters and evaluating the performance of machine vision systems where it is too expensive or not possible to acquire actual test images. MOC2DIMES uses as inputs images from orbit of candidate Mars landing sites, lander descent profiles and operating conditions, fixed camera parameters and calibration data, and produces geometrically and radiometrically accurate descent camera images. The images generated include a full range of descent dynamics, planetary terrain effects, and non-ideal camera behaviors. This paper describes the MOC2DIMES simulator and shows how it was used to develop the velocity estimation algorithm used in the Mars Exploration Rover (MER) Descent Image Motion Estimation System (DIMES).

1. INTRODUCTION

DIMES was added to the MER landers to estimate the horizontal velocity of the spacecraft during terminal descent. The system uses a $45 \times 45^\circ$ FOV downward looking camera on the lander to acquire three images in the last 2000 meters of descent, track features in these images, and thereby estimate the horizontal velocity of the descending spacecraft [1]. The horizontal velocity estimates in turn are used by firing control logic in the landing rocket system to reduce the horizontal velocity of the spacecraft before touchdown.

MOC2DIMES was developed to generate images similar to those the descent camera would produce for MER landing sites and conditions, enabling realistic testing and tuning of the DIMES algorithms. The simulator incorporates important nominal camera behaviors, terrain effects and descent dynamics effects. It also models off-nominal effects such as dust contamination to support sensitivity analysis.

Versions of MOC2DIMES were used from early proof-of-concept through development and final landing site selection.

2. MOC2DIMES INPUT AND OUTPUT DATA

Each MOC2DIMES simulation run starts with a camera configuration, a descent profile and a terrain image and produces three descent camera images and lander state data for input into DIMES.

2.1 Camera configuration

The camera configuration describes the fixed geometric, radiometric and electrical characteristics of the DIMES camera system being simulated.

The geometric characteristics are contained in machine vision camera models [2] calibrated from test bed and flight hardware. The models include the 3D scene to 2D image projection (including geometric distortion) and the geometric transform between the camera and lander coordinate frames.

The camera's radiometric characteristics are contained in models of optical intensity ($\cos^4\theta$) falloff with field angle, θ , measured from the optical axis, relative CCD Pixel Response Non-Uniformity (PRNU), and an absolute radiance-to-photo-electron (signal) photo response value calibrated from test bed and flight cameras.

The electrical characteristics of the cameras are contained in a dark current model calibrated during CCD characterization and analog-to-digital (ADC) conversion performance parameters including the ADC gain and the readout and quantization noise statistics determined during camera development and calibration.

2.2 Descent profiles

Descent profiles provide the descent dynamics and conditions for a MOC2DIMES simulation run. Scenarios are based on Automated Dynamic Analysis of Mechanical Systems (ADAMS) multi-body simulations for the lander and include altitudes, velocities, angular attitudes and rates, and horizontal steady state winds experienced by the lander. Descent profiles can also come from the Program to Optimize Simulated Trajectories (POST) [3].

2.3 Terrain images

In MOC2DIMES, terrain images are projected into the descent camera field of view to produce the initial appearance of the landing site.

The Mars Global Surveyor (MGS) Mars Orbiter Camera (MOC) Narrow Angle (NA) instrument is a 35 cm aperture, 3.5 m focal length, $f/10$ telescope with a 0.4° FOV and spectral sensitivity from 500-900 nm. The focal plane contains a 2048 element, $13\ \mu\text{m}$ pixel CCD line array [4]. During the period leading up to the Mars Exploration Rovers (MER) mission, the MOC took images of the candidate MER landing sites as an important input to the final site selections.

We selected images from this MOC data set to optimize and test DIMES performance after processing the MOC images through the MOC2DIMES camera simulator. MOC images selected for this purpose had incidence and phase angles $< 60^\circ$ and emission angle $< 30^\circ$, spatial resolution $\sim 3\ \text{m/pixel}$, and cross-track width of the MOC image strip $\sim 3\ \text{km}$. The expected DIMES image parameters were $5\ \text{m/pixel}$ resolution and 18° - 33° incidence angle. The width of each image strip was at least twice the DIMES FOV and many DIMES test runs were possible within the area covered by a single MOC image strip

Each MOC image was reduced to absolute I/F (reflectance) values by USGS Flagstaff personnel using the Integrated Software for Imagers and Spectrometers (ISIS) system (K. Herkenhoff, personal communication). For a given descent profile, these I/F values were converted to a corresponding radiance image of the Mars scene that was then input to the DIMES camera model, as described in section 3.1.

To account for the different spectral sensitivities of the MOC and DIMES cameras we determined the ratio of the camera responses for the sun spectra and an average spectral reflectance profile for Martian soil [5] and applied it to the overall radiance field.

The availability of meter scale resolution MOC images of the actual Mars landing site areas was a valuable resource for DIMES testing and optimization. But because MOC always viewed Mars surface through a long path of fine dust suspended in Mars' thin atmosphere, contrast in the test images was reduced and represented a worst case scenario. We anticipated that due to the difference in altitude of DIMES and MOC above Mars' surface, the optical depth of dust would be a factor of ~ 8 times less for DIMES. To be conservative we did nothing to compensate for this.

MOC images included shot noise which appeared as an artificial fine grain texture or contrast not found on the actual terrain. Image smoothing introduced by the bilinear interpolation used for image reprojection and scaling at each new camera position plus the

uncorrelated shot noise added to each image by the camera simulator eliminated the chance DIMES would correlate on the texture rather than on terrain features.

2.4 Outputs

MOC2DIMES produces three geometrically and radiometrically accurate 1024×256^1 pixel 12-bit images for each descent profile. Included with each image is the lander attitude, angular rate and radar altitude that would have been measured by the flight system when each image was captured. The simulator also outputs the horizontal steady state wind velocity from the descent profile for use as ground truth for comparison with the velocity estimate produced by DIMES. Fig. 1 shows a typical descent camera image generated by MOC2DIMES.



Fig. 1. Typical MOC2DIMES descent camera image.

3. MODELLED EFFECTS

A particular concern for DIMES was the low contrast provided by MER landing site terrain and as a consequence, the potential sensitivity of the DIMES algorithm to nominal but non-ideal camera and scene effects. MOC2DIMES models the most significant of these effects. It also models off-nominal camera effects to help characterize the algorithm's sensitivity and robustness.

3.1 Camera effects

The DIMES camera is a 14.67 mm focal length, $f/12$ camera with a $45 \times 45^\circ$ FOV and spectral response from 400-1100 nm. The focal plane is a 1024×1024 , $12\ \mu\text{m}^2$ pixel frame transfer CCD [6].

Several non-ideal camera effects, such as radial lens distortion, relative intensity fall off with field angle, PRNU, dark current signal, CCD readout noise and ADC quantization noise, are independent of the scene being imaged and are handled by MOC2DIMES as fixed calibration data as described in section 2.1.

Other non-ideal camera effects such as fast flush and frame transfer image smear and pixel shot noise are scene dependent and must be recalculated by MOC2DIMES during each simulation run.

¹ Descent camera images are binned down from 1024×1024 to 1024×256 inside the camera to reduce the image readout time.

Fast flush and frame transfer image smear arise in the DIMES camera because the radiance field formed by the camera lens is constantly generating charge in the CCD's active area during all phases of image capture including pre-integration array clearing (fast flush) and post-integration array storage (frame transfer). For DIMES the fast flush, image integration and frame transfer times are all 5.1 ms so the extra charge added to the image pixels as they are shifted across the CCD during fast flush and frame transfer represents a significant added bias noise in the final image. MOC2DIMES models fast flush and frame transfer image smear by computing the additional charge each image pixel receives from each part of the radiance field as the pixel is shifted across the CCD during fast flush and frame transfer.

Shot noise arises in pixels because photo and thermally generated electrical current is carried by discrete charges. Shot noise is a Poisson process and the charge carriers that make up the current will follow a Poisson distribution. MOC2DIMES models shot noise by treating the total number of photo and thermally generated electrons accumulated in a pixel during the simulation as a mean value. The "true" number of electrons for the pixel is drawn from a Poisson distribution with mean and variance equal to this accumulated value.

3.2 Descent scenario effects

We used the MOC images to extensively test, refine and optimize DIMES to reliably estimate the horizontal velocity of the lander through near-real-time image analysis. However, important differences between the MOC NA images acquired from orbit and the DIMES images that would be acquired with small aperture (1 mm), wide angle (45° FOV, $f/12$) optics from very low altitude (2000 m) had to be modeled before testing on realistic simulated DIMES images was possible.

The small angular FOV of the MOC NA camera means that the emission angle (defined at the pixel location on Mars' surface as the angle between the surface normal and the vector to the camera) and the phase angle (the angle between the vector to the sun and the vector to the camera) for all of the pixels in a landing site image change very little across the MOC image. But in the wide-angle DIMES image, both the emission and phase angles can vary by as much as 45° within a single image.

Because the reflectance of the surface is a function of the emission and phase angle, the MOC images must be radiometrically corrected to account for these variations.

This "radiometric correction" used a simple photometric function applicable to planetary surfaces with reflectance < 0.5,

$$I/F = [\mu_0/(\mu+\mu_0)] f(\alpha) \quad (1)$$

where I is the radiance of the surface, πF is the incident solar irradiance normal to the sun-vector, α is the phase angle, and μ and μ_0 are the cosines of the emission and incidence angles, respectively [7]. For Mars we used,

$$f(\alpha < 10^\circ) = 2.05 - (3.93e-2)\alpha + (2.09e-3)\alpha^2 - (4.86e-5)\alpha^3 + (4.93e-7)\alpha^4 - (1.72e-9)\alpha^5 \quad (2)$$

$$f(10^\circ > \alpha > 60^\circ) = 1.82 - (1.03e-2)(\alpha-10^\circ) \quad (3)$$

which we derived from analysis of MOC wide-angle images for $\alpha < 10^\circ$ and from many MOC NA images for $10^\circ > \alpha > 60^\circ$.

The main effect of this correction is to create a bright "halo" around the point where the projection of the vector from the sun through the lander intercepts Mars' surface in the corrected image (Fig. 2), the "opposition effect" well-known to planetary astronomers. The shadow of the lander and its large parachute are at the center of this bright spot. Because this combination results in a high-contrast feature that is not fixed on the surface, DIMES identifies a 4.3° half angle zone around the center of the bright spot and excludes it from the feature tracking analysis used to determine horizontal velocity.

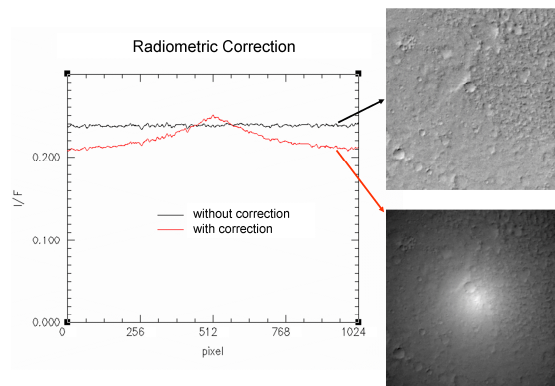


Fig. 2. Opposition effect in radiometrically corrected MOC image.

Although we did not simulate 3D terrain relief and shadowing with MOC NA images, these effects were determined to not have a large effect on DIMES performance given the high altitude and relatively flat landing sites. Furthermore, field testing over Mars-like terrain [8] showed that even with large terrain relief, the DIMES algorithm still met its accuracy requirement of 5 m/s.

Since MER's descent dynamics might include angular rotations up to 60 degrees per second and the descent camera had a 5.1 ms exposure time, MOC2DIMES needed to simulate motion induced image blur. MOC2DIMES incorporates motion blur into the fast flush, exposure, and frame transfer integrations by generating multiple incident radiance fields for the positions and attitudes that occur along the descent profile during each integration period. New radiance fields are generated in steps corresponding to one MOC pixel of image shift. The radiance fields (typically from two to four) are then averaged on a pixel by pixel basis to generate a blurred image of the terrain.

While heat shield separation on MER occurs several seconds before DIMES takes its first image, the trajectory of the heat shield is not well understood and there is a finite chance the heat shield could appear in one or more of the descent camera's images. To be conservative MOC2DIMES models a worst case trajectory putting the heat shield at closest separation and slowest velocity. The heat shield's appearance is modeled as a 5.3 m diameter 140° cone with the surface reflectance properties we measured for the carbon-impregnated black Kapton thermal blanket that lines the heat shield's interior.

3.3 Off-nominal camera effects

One concern for DIMES was that particulate debris floating loose in the spacecraft or generated by the pyrotechnics used for heat shield separation might end up on the front of the descent camera optics causing image artifacts that would defeat or spoof DIMES. To assess the potential impact of this MOC2DIMES includes a dust artifact model [9] that can simulate image artifacts for a random number of random sized particles distributed randomly on front surface of camera.

4. SIMULATION FLOW

MOC2DIMES camera simulation is done in two stages: scene modeling and camera modeling. Scene modeling (Fig. 3) takes raw MOC NA reflectance images and converts them into the radiance field the DIMES camera would see while looking down at the terrain. Camera modeling (Fig. 4) converts the radiance field seen by the camera into the final 12-bit/pixel DIMES camera images.

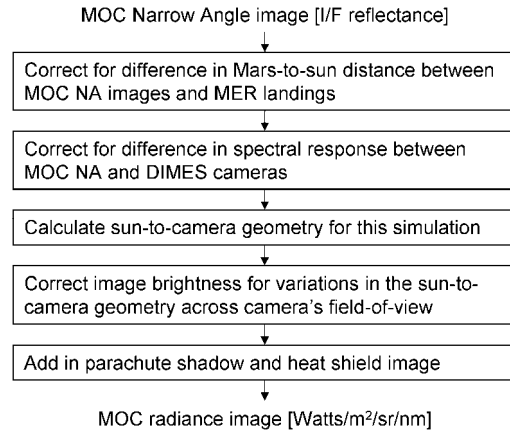


Fig. 3. MOC2DIMES scene modeling flow.

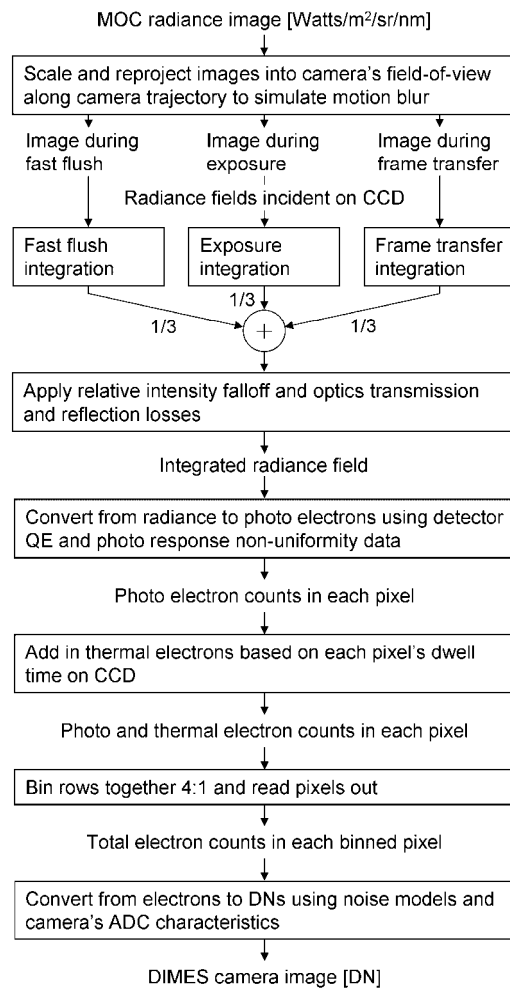


Fig. 4. MOC2DIMES camera modeling flow. DN are Data Numbers or greyscale values.

5. DIMES ALGORITHM TESTING

Validation of the performance of DIMES was critical to prove that DIMES would “do no harm” during Entry Descent and Landing (EDL). Because the entire DIMES flight system could not be tested completely in a realistic flight like environment, the validation tests were broken into three categories. Flight system testing proved that the flight software worked on the flight system and that the DIMES velocity answer was available in time to effect RAD fire. Field testing proved that the camera and algorithm would produce reasonable velocity estimates when imaging Mars like terrain at representative altitudes [8]. In addition, during the development process Monte Carlo simulation with MOC2DIMES was used to estimate the statistical performance of DIMES at each landing site under realistic EDL dynamics and images of actual Martian landscapes. It was also used to investigate algorithm sensitivity to non-ideal and off-nominal imaging effects.

MOC2DIMES inputs were set based on the MER EDL environment. Multi-body aerodynamic simulations of the lander system were used to generate EDL trajectories [3]. Flight system testing was used to determine the typical altitude of the first image exposure (2000 m) and the time between the second and third images (3.75 s). This information was used to look up the true camera state in each EDL trajectory. Representative values were:

- Altitudes: 2000 m, 1725 m and 1450 m
- Attitude: off nadir angle $< 30^\circ$ and roll $< 45^\circ$
- Angular rates: $< 60^\circ/\text{s}$
- Velocity: vertical ~ 72 m/s and horizontal < 30 m/s
- Position of heatshield relative to lander: 140-200 m axial separation, 50-75 m lateral separation.

Each MOC image is bigger than a set of descent images, so multiple simulation test cases can be created from each by placing the EDL trajectory at different locations across the MOC image. The constraints for placing the trajectories are that each descent image must stay within the horizontal bounds of the MOC image and that the trajectories should evenly sample the appearance of the MOC image so that DIMES performance statistics are not biased. Fig. 5 shows an example of image states from three trajectories and associated fields of view on a MOC image.

The internal camera model parameters (e.g., I/F to photoelectron scale factor, dark current, PRNU, projection model, radiometric fall off) were set based on calibration data from the MER DIMES flight cameras. The expected operating temperature was -20°C , but, to be conservative, the CCD temperature was set to 0°C .

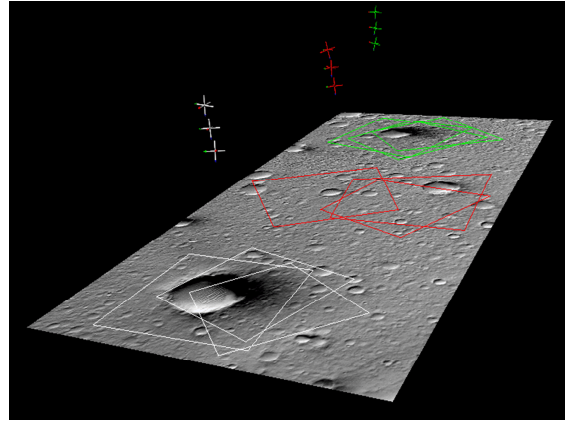


Fig. 5. Representative EDL trajectories (+) and DIMES camera fields-of-view (polygonal boxes), projected within a MOC image.

Besides the descent images, the DIMES algorithm also requires estimates of lander attitude, altitude, and biased horizontal velocity. Sensor models were used to generate these measurements, including noise, from the true EDL trajectories that were used to generate the images. Attitude errors, including absolute biases ($\sigma=1^\circ$), between image random errors due to timing accuracy ($\sigma=0.05^\circ$), and alignment accuracy ($\sigma=0.1^\circ$), were based on EDL requirements. Altitude errors were based on the measured performance of the radar altimeter ($\sigma=0.03\%$ of altitude).

All Monte Carlo simulation test cases are generated by selecting a MOC image and an EDL trajectory. The trajectory is placed on the MOC image and the descent images are simulated with MOC2DIMES. Noisy sensor measurements are generated and the images and noisy measurements are input into the DIMES flight software [1] to generate a velocity estimate and a valid velocity flag. This process is repeated multiple times to generate statistical assessments of velocity estimation accuracy and percent valid velocities reported.

Each MER landing site was imaged by MOC multiple times for landing site selection and hazard assessment. The DIMES simulation used the subset of these images that had photometry similar that expected during landing. MOC images and associated coverage for each of the landing sites are given in Figs. 6 and 8.

Terrain appearance has a strong influence on DIMES performance; the number of valid velocities will decrease as the terrain becomes blander. Both of the MER landing sites had wide variability in appearance. To capture this variability in performance each landing site was manually segmented into “appearance classes” based on orbital images (Figs. 7 and 9). Each landing

site had three appearance classes which covered different fractions of each landing ellipse.

The Monte Carlo simulation of DIMES performance proceeded as follows for each landing site. First, the camera parameters specific to the flight camera for the landing site (MER-A or MER-B) were input into MOC2DIMES. Next, the MOC images for each appearance class were selected. Then for each MOC image from the appearance class, a set of EDL random pregenerated trajectories specific to the landing site (the trajectories for Gusev Crater had more winds and greater attitude excursions) were selected and placed to cover the image. These trajectories also included the position of the heatshield relative to the lander. Descent images and sensor measurements were generated for each trajectory and fed into the DIMES flight software. The velocity estimation results were then added to the results for the current appearance class. This process was repeated for each appearance class. The final result for each landing site was then created by taking an ellipse fraction weighted sum of the results from each appearance class.

Tables 1 and 2 show the simulated performance of DIMES at Gusev Crater and Meridiani Planum. The DIMES software parameters were fixed for each landing site, but tuned to Gusev where there is more scene contrast and also more winds. These conservative parameters are the reason for the decrease in the valid velocity percentage at Meridiani Planum. If the parameters had been tuned to Meridiani, the valid velocity percentage would have been greater than 90%. The velocity accuracies are for an altitude of approximately 1600 m.

MOC2DIMES was also used to test velocity estimation performance sensitivity to a number of off nominal conditions including high motion blur, excessive dark current and spikes, dust particles on the lens, specular reflections and blooming off of the heatshield and energetic particle hits.

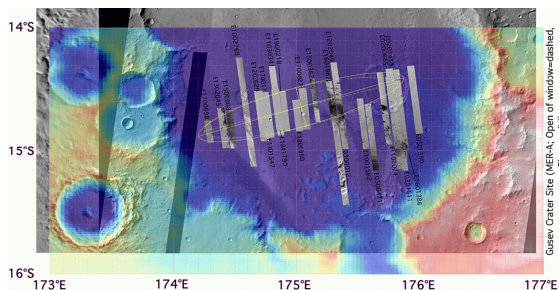


Fig. 6. Gusev Crater MOC coverage (52%). (Image courtesy Tim Parker / JPL).

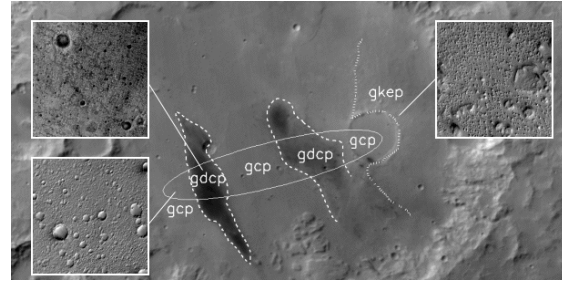


Fig. 7. Gusev Crater appearance class coverage. **gcp**: Gusev cratered plains – higher albedo, smooth plains with few craters, bright crater rims, and low contrast overall (ellipse fraction = 59%). **gdcp**: Gusev dark cratered plains – lower albedo, mostly due to linear dark dust devil tracks, cratered plains area (ellipse fraction = 41%). **gkep**: Gusev knobby etched plains – knobs or mesas of positive relief dominate this area surrounding crater at east end of ellipse (ellipse fraction = 0%).

Table 1. Gusev Crater MOC2DIMES performance.

| Appearance Class | Number of Cases | Number of valid cases | % valid | Velocity Error (m/s) (mean + 3 sigma) | % landing ellipse | Weighted % Valid | Weighted Velocity Error (m/s) (mean+ 3 sigma) |
|------------------|-----------------|-----------------------|---------|---------------------------------------|-------------------|------------------|---|
| gcp | 186 | 182 | 98% | 3.90 | 59% | 58% | 2.30 |
| gdcp | 112 | 112 | 100% | 3.48 | 41% | 41% | 1.43 |
| gkep | 78 | 77 | 99% | 3.29 | 0% | 0% | 0.00 |
| Gusev | 376 | 371 | | | | 99% | 3.73 |

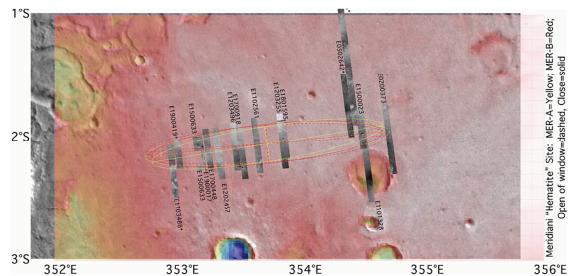


Fig. 8. Meridiani Planum MOC coverage (31%). (Image courtesy Tim Parker / JPL).

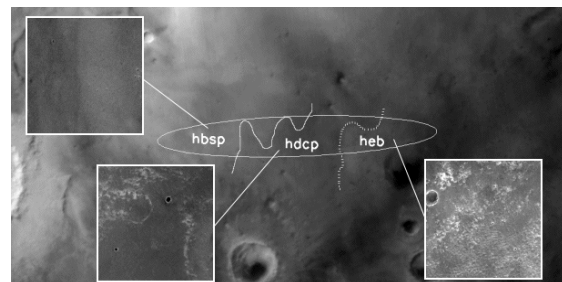


Fig. 9. Meridiani Planum Appearance Class Coverage. **hbcp**: Hematite bright smooth plains – higher albedo, smooth plains with few craters, low contrast (ellipse fraction = 34%). **hdcp**: Hematite dark cratered plains – lower albedo, cratered plains (ellipse fraction = 40%). **heb**: Hematite ejecta blanket – ejecta apron surrounding large crater near east end of ellipse (ellipse fraction = 26%).

Table 2. Meridiani Planum MOC2DIMES performance.

| Appearance Class | Number of Cases | Number of valid cases | % valid | Velocity Error (m/s) (mean + 3 sigma) | % landing ellipse | Weighted % Valid | Weighted Velocity Error (m/s) (mean + 3 sigma) |
|------------------|-----------------|-----------------------|---------|---------------------------------------|-------------------|------------------|--|
| hbsp | 44 | 22 | 50% | 4.06 | 34% | 17% | 1.38 |
| hdcp | 179 | 125 | 70% | 3.92 | 40% | 28% | 1.57 |
| heb | 31 | 31 | 100% | 3.03 | 26% | 26% | 0.79 |
| Meridiani | 254 | 178 | | | | 71% | 3.74 |

6. MER RESULTS

After both landings, the DIMES descent images, state measurements and algorithm results were sent back to Earth. In the case of MER-A, which landed in Gusev Crater, a MOC image that covered the MER-A landing site had already been taken before landing. Using this MOC image, the state measurements and the velocity computed on-board, it was possible to create MOC2DIMES images that matched the viewing conditions of the MER-A descent images.

Fig. 10 shows the first simulated MOC2DIMES image and the image collected by the DIMES camera during flight (both images scaled between 1200 and 200 DN). The top row of Fig. 12 shows these simulated images after they have been binned to 256x256 and had the radiometric fall-off, fast flush and frame transfer removed. As the figures show, the images are similar in both the raw and flattened versions, but the MOC2DIMES image is brighter and has less contrast than the MER-A image.

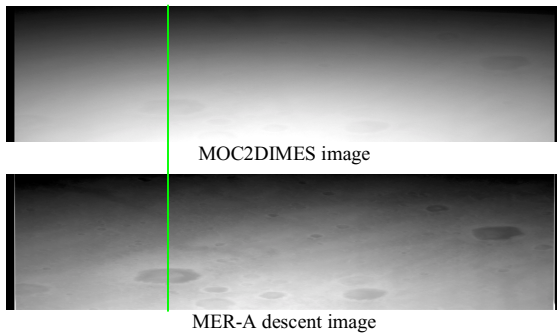


Fig. 10. Comparison of MOC2DIMES image of MER-A landing site to actual MER-A descent image. Upper right corner of MOC2DIMES image has no texture because image field of view went outside MOC image. Green line indicates columns plotted in Fig. 11.

Fig. 11, which plots a column from each of the raw images, helps explain these differences. Both column plots show the frame transfer ramp. The MOC2DIMES pixels have a higher DN values than the MER-A image while the MER-A pixels vary more indicating a higher level of scene contrast. By plotting a scatter plot of one column vs. the other (Fig. 11, right), it is easy to see that the data are highly correlated (correlation coefficient of 0.99) which indicates that over the entire column, the images are similar up to a constant scale factor indicated by the

slope of the scatter plot ($m=0.85$). This 15% difference encompasses all possible error sources including MOC image I/F calibration, camera radiometric calibration and scene photometric effects.

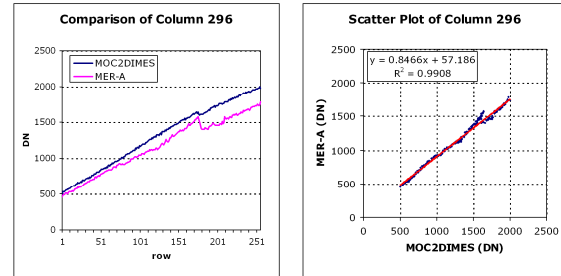


Fig. 11. (left) Comparison of column 296 from MOC2DIMES and MER-A image shown in Fig. 10. (right) Scatter plot of columns 296 and associated best fit line and correlation coefficient.

A high level way to compare MOC2DIMES to MER-A is to compare the results produced by the DIMES flight software run on both sets of images. Fig. 12 compares the features selected in the first and second MOC2DIMES images to the features selected in the first and second MER-A images. Three out of four of selected templates are the same. This is one indicator that the images produced by MOC2DIMES will produce comparable velocity estimation results to those seen in flight. Table 3 compares some of the DIMES correlation metrics [1] for these three similar templates. As discussed previously, the MOC2DIMES templates are brighter (5% to 15%) while the MER-A templates have higher contrast. (3x). Even with the decrease in contrast, the MOC2DIMES and MER-A templates have similar correlation coefficient indicating that the velocities computed with MOC2DIMES are as reliable as the velocities computed in flight. This result confirms that MOC2DIMES was an accurate tool for assessing DIMES performance.

The loss of contrast in MOC2DIMES was expected. During field testing, it was discovered that the contrast of the field test imagery was significantly higher than that seen in MOC2DIMES. It was determined that this discrepancy was caused by MOC viewing the Martian surface through the entire dusty atmospheric column as opposed to just 2 km of atmosphere encountered during field testing and flight.

Fig. 13 shows the first and third images from the MER-B landing. The first image shows the heatshield as a black spot falling to the surface during descent. The third image clearly shows the parachute shadow and the zero phase opposition effect around the shadow. As described above, all of these effects were modeled in MOC2DIMES and as the pictures indicate, it was important to do so.

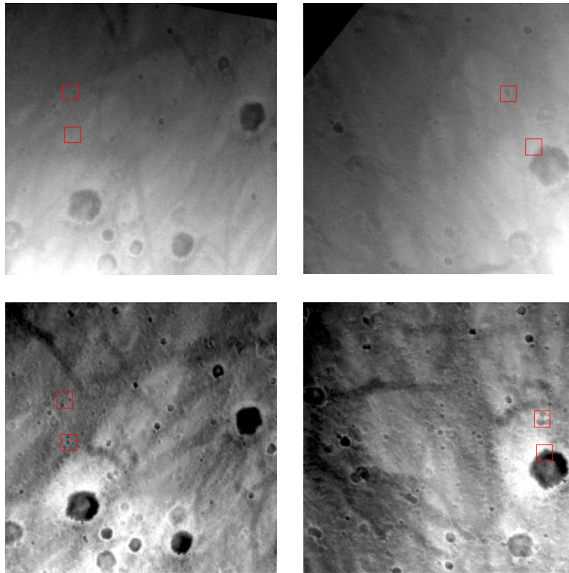


Fig. 12. Comparison of features selected by DIMES flight software in MOC2DIMES images (top row) compared to features selected in flight during MER-A (bottom row).

Table 3. Comparison of correlation metrics from DIMES flight software for MOC2DIMES (M2D) and MER-A.

| | Brightness | | Contrast | | Correlation | |
|------------|------------|------|----------|------|-------------|------|
| | M2D | MER | M2D | MER | M2D | MER |
| Feature 00 | 5212 | 4710 | 14.9 | 47.5 | 0.87 | 0.88 |
| Feature 01 | 4139 | 3898 | 14.1 | 41.7 | 0.84 | 0.91 |
| Feature 10 | 5526 | 4693 | 23.1 | 55.6 | 0.94 | 1.00 |
| Feature 11 | N/A | | | | | |

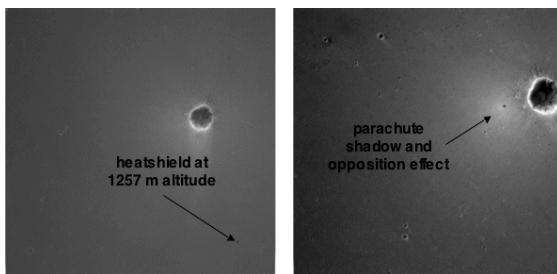


Fig. 13. MER-B descent images showing heatshield, parachute shadow and opposition effect.

7. CONCLUSIONS

MOC2DIMES was an indispensable tool in the development of the MER DIMES system. It enabled validation and characterization of DIMES performance and robustness to a degree that could not have been done any other way. It helped provide enough confidence in DIMES and the wind tolerance of the landing system for the project to choose Gusev Crater

as a landing site. In the end DIMES performed flawlessly at both landing sites, and in the case of MER-A, enabled the landing system to reduce the horizontal touchdown velocity from the edge of its design limits to a level well within its capability.

8. ACKNOWLEDGMENTS

The research described in this paper was carried out at the Jet Propulsion Laboratory, California Institute of Technology, under a contract with the National Aeronautics and Space Administration.

9. REFERENCES

- Cheng Y., Johnson A.E., and Matthies L.H., *MER-DIMES: A Planetary Landing Application of Computer Vision*, IEEE Conference on Computer Vision and Pattern Recognition (CVPR 2005), June 2005.
- Gennery D.B., *Least-Squares Camera Calibration Including Lens Distortion and Automatic Editing of Calibration Points*, in Calibration and Orientation of Cameras in Computer Vision by Springer-Verlag, A. Gruen and T. Huang editors, Berlin, 2001.
- Raiszadeh B., and Queen E.M., *Mars Exploration Rover Terminal Descent Mission Modeling and Simulation*, Paper AAS-04-271, AIAA Space Flight Mechanics Meeting 2004.
- Malin M.C., et al., *The Mars Observer Camera*, J. Geophys. Res., 97 (E5), 7699-7718, 1992.
- Maki J.N., et al., *The color of Mars: Spectrophotometric measurements at the Pathfinder landing site*, J. Geophys. Res., 104(E4), 8781, 1999.
- Maki J.N., et al., *Mars Exploration Rover Engineering Cameras*, J. Geophys. Res., 108(E12), 8071, 2003.
- Buratti B.J., *Voyager Disk Resolved Photometry of the Saturnian Satellites*, Icarus 59, 392-405, 1984.
- Johnson A.E., et al., *Field Testing of the Mars Exploration Rovers Descent Image Motion Estimation System*, IEEE International Conference on Robotics and Automation, (ICRA 2005), April 2005.
- Willson R.G., Maimone M.W., Johnson A.E., and Scherr L.M., *An Optical Model for Image Artifacts Produced by Dust Particles on Lenses*, 8th International Symposium on Artificial Intelligence, Robotics and Automation in Space, September 2005.